University of South Wales

Transfer Report

Sebastian Haigh

12035262

October 2017

Director of Studies: Dr. Janusz Kulon
Supervisor: Dr. Peter Plassmann
Company Advisor: Prof. Colin Gibson

Abstract

This report presents the work that has been done to date in the development of an anatomical landmark localisation system. The system is being developed as an improvement to existing methods for postural assessment of individuals with complex needs.

The device that is being developed is a 3D ultrasonic positioning system, using a number of transmitters to emit acoustic signals that are recorded by an ultrasonic microphone. The data obtained from this can be used to calculate the 3D position of the microphone. In order to be practical, this device will need to be able to cope with complicated situations including reception of reflected signals and the possibility of signal blockage due to obstacles while still providing accurate position information.

A novel technique for overcoming the effect of reflected signals has been developed, which exhibits good performance at classification and rejection of reflected signals, while outperforming state of the art techniques in terms of computational cost. This technique has been tested on data collected during experiments.

Further work has been planned, including modification of the reflection rejection technique to also overcome the effects of obstacles. This plan has been presented along with a time-scale for its completion within the next year.

Contents

Nomenclature

$\mathbb{R}$	The set of all real numbers
$\nabla f(x)$	Gradient of a function $f(x)$
$\nabla^2 f(x)$, $\mathbf{H}_f(x)$	Hessian matrix of a function $f(x)$
$\mathbf{J_r}(x)$, $\mathbf{J_r}$	Jacobian matrix of a vector valued function $\mathbf{r}(x)$
k	Transmitter index
m	Number of transmitters
$t_{0\|k}$	Time of the beginning of signal transmission from the k^{th} transmitter
$t_{A\|k}$	Time the signal from k^{th} transmitter arrives at the receiver
$t_{F\|k}$	Time of flight of the signal travelling between the k^{th} transmitter and the receiver
x_k, y_k, z_k	Cartiesian coordinates of the k^{th} transmitter

Bayesian Probability

$\hat{\phi}$	Estimate of class membership
$\hat{\phi}^{-}_{b_k\|s_i}$	Estimate of class of signal i in block k based only upon information regarding block k
ϕ	Class membership
A	Event - signal is LoS
A^*	Event - signal is NLoS
i	Index of received signals
$p(s_i\|A)$	Probability of signal being LoS

Nonlinear Regression

$\hat{\mathbf{x}}$	Estimated position of the receiver in vector form
λ	Levenburg-Marquart parameter
$\mathbf{r}(\hat{\mathbf{x}})$	Residual vector
$\mathbf{x}_k$	Position of k^{th} transmitter in vector form

Chapter 1

Introduction

Individuals with severe musculoskeletal deformities often require custom contoured wheelchair seating, this is important for comfort, proper breathing and for preventing the worsening of their condition. In order to design and manufacture such seating, the individual must first undergo a process of postural assessment.

Tools exist for performing such assessments in a non-invasive fashion, such tools are generally limited to measuring a particular part of the spine, or measuring in a particular anatomical plane. Examples include the flexible ruler [1], the arcometer [2, 3], the kyphometer [4], amongst others [5], however these tools and methods are not well suited to individuals with complex needs, whose anatomy falls so far from the norm that any general purpose tool is very limiting. As such, obtaining an accurate representation of the individuals spine shape via currently existing non-invasive methods is very difficult, time-consuming and costly.

Radiographic techniques yield very accurate data, however due to factors such cost cost and ease of access to the proper equipment, these methods are not practical for use in postural assessment in a clinical environment. They also expose the individual to high levels of radiation. Due to the frequency at which such individuals must be assessed, the use of radiographic methods can lead to detrimental side effects caused by repeated exposure to radiation. It is, therefore, highly desirable to avoid any techniques which involve radiation.

The goal of this project is the creation of a new tool capable of capturing the position of anatomical landmarks as points in the three dimensional Eucildiean space $\mathbb{R}^3$. Such points can be collected for multiple landmarks and input to an inverse kinematic digital human model (DHM), which would yield a good estimate of the spine shape.

This tool should allow the assessment to be conducted quickly and intuitively without the need for lengthy and invasive procedures and without exposing the individual to any quantity of radiation.

This new tool will be an ultrasonic positioning system, with transducers embedded in a glove, allowing for the localisation of fingers and hands of the clinician. Such a device would allow the process of palpation to be directly tracked.

Acoustic signals have many advantages that make them attractive for use in indoor positioning and measurement systems. These signals are non-invasive, have no effect on human physiology and can not be detected by human senses. As such they are not harmful nor do they cause additional discomfort.

Due to the relatively slow speed of sound in air, these signals allow for better estimates of distance travelled than radio frequency signals which travel at the speed of light.

Using ultrasonic localisation techniques to perform localisation in a clinical setting poses several significant challenges. The performance of such acoustic methods is highly sensitive to interference from the environment, in the form of reflected signals and blocked signals. Both of these situations can lead to a failure of the standard techniques for calculation of the 3D position, this is due to a lack of information in the case of signal blockage and due to invalid information in the case of reflection. In order to ensure the practicality of this device, these standard algorithms must be made robust to the effects of reflection and signal blockage.

1.1 Aim & Objectives

The aim and objectives of the project are summarised below.

Aim

• Development of 3D anatomical landmark localisation system using acoustic emission.

Objectives

• Data will be collected from ultrasonic localisation experiments that simulate forms of environmental interference.
• Algorithms will be developed to make the localisation process robust to environmental interference.
• Algorithms will be tested and validated against data collected from experiments.
• A prototype will be developed of the complete system including glove with embedded transmitter.
• Prototype system will be tested and validated using a phantom model of a human spine.

1.2 Original Contributions to Knowledge

To the best of the author's knowledge, there does not currently exist any anatomical landmark localisation device using ultrasonic acoustic emission to directly track and record palpation. The process of developing this novel device generates multiple opportunities for original work and it is predicted that this research will produce the following original contributions to knowledge:

1. Development of a reflection classification and rejection technique using Bayesian probability and iteratively reweighted least square regression.
The possibility of reflected acoustic signals is a major disadvantage in ultrasonic localisation. In working towards the completion of this project a technique has been developed that uses a combination of Bayesian probability and iteratively reweighted least squares regression to classify and reject reflected ultrasonic signals. This method is capable of overcoming the problem of reflected signals with a far lower computational cost than the state of the art techniques presented in the literature.

2. Development of a method for robustly overcoming the effects of signal blockage.
Another major disadvantage in ultrasonic localisation is the possibility of obstacles blocking the travel of the acoustic signals. This especially problematic in the application of postural measurement since, in order to take measurements, a clinician will need to be positioned somewhere in the space between the transmitters and the individual being assessed. A method is required to compensate for these effects, the reflection rejection technique already developed

3. Validation of reflection rejection & signal blockage mitigation methods against experimental data.
The methods developed for overcoming the disadvantages of ultrasonic localisation will be tested against experimental data. This data was recorded during two separate experiments, each of which used different configurations of the system by varying different experimental parameters including: sample rate, number transmitters and their positions, position of receivers, orientation angle of receivers with respect to the transmitters and the envelope of output signals.

In addition to investigating the effects of different configurations, these experiments also focused upon the effects of environmental interference. This was achieved by the introduction of different sources of interference, *i.e.:* highly reflective materials and objects block the direct line of travel of the acoustic signals. The effects of the environmental interference will be analysed against baseline measurements conducted without the interference present. The analysis of this data will provide a detailed insight into the effect of such interference. The data itself will also be used to validate the performance of the methods described in points 1 & 2 in a variety of challenging situations.

4. Determining the appropriate configuration of hardware for anatomical landmark localisation
Ultrasonic localisation systems have many applications, such as indoor positioning and mapping, however different systems require different configurations of the component parts of the system, and other hardware considerations such as the minimum required sampling rate. Since the use of an 3D ultrasonic localisation system to track and record palpation does not exist, it has not been determined what configurations will

give adequate performance for this purpose. This information can be determined from a detailed analysis of the experimental data that has already been obtained, and that will be obtained from future experiments.

5. Integration of an ultrasonic localisation system into a wearable device for estimation and recording of 3D position

The system developed will need to be transferred into a novel wearable device that allows for the position of the fingertips of the wearer to be tracked and recorded. This will require the design of such a wearable device that allows all of the required sensors to be embedded into a glove, while not constricting the normal movement of the hand nor impeding the normal work of the clinician.

6. Validation of the 3D ultrasonic localisation system for use in postural assessment. The prototype system will to tested using a phantom model of a human spine. The system will be used to measure anatomical landmarks on the phantom model and the estimated positions recorded, these measurements can then be validated by comparing them to measurements made by a coordinate measuring machine. The performance of the ultrasonic system for anatomical landmark localisation can then be assessed and evaluated and a determination made regarding the devices suitability for this purpose.

Chapter 2

Literature Review

2.1 Introduction

The chapter provides a condensed review of literature in the area of ultrasonic localisation, primarily focusing upon the state of the art in reflection rejection and mitigation techniques. The author has chosen to limit the scope of this review to focus mainly on this area since it relates most to work that has been done so far, in order to balance the needs to fully address the subject with consideration for the length of the report.

2.2 Ultrasonic Measurement - Background Theory

An ultrasonic localisation system consists, mainly, of m transmitting beacons in known locations and a receiver in an unknown location.

The each of the m beacons transmit bursts of ultrasound at time $t_{0|k}$. These bursts propagate through the air and arrive at the receiver at a time $t_{A|k}$. The time of arrival, $t_{A|k}$ and the time of transmission, $t_{0|k}$, can be used to calculate the time of flight, $t_{F|k} = t_{A|k} - t_{0|k}$.

The distance travelled by the acoustic signal is thus $d_k = ct_{F|k} = c(t_{A|k} - t_{0|k})$, where c is the speed of sound in air.

2.2.1 Time of Arrival & 1D Distance Estimation

Accurately estimating the time of arrival is key to obtaining accurate distance measurements d_k, since the d_k's are calculated from the time of arrival. Furthermore, since the 3D position is synthesised from multiple

distance measurements, it can be seen easily that any error in estimation of the time of arrival will propagate through the entire process and create errors in the 3D position estimation. Time of arrival estimation is, therefore, and important consideration and receives much attention in the literature.

Detecting the exact arrival time is challenging, since the beginning of the signal will often be buried in noise or obscured by overlapping, reflected signals.

As such there are many methods of estimating time of arrival of the signals such as those presented in [6, 7, 8, 9]. These techniques have differing accuracy and are intended for a range of different applications, from the large scale systems with errors in the range of 0.5 metres to 1.5 metres to far more precise systems reporting submillimeter accuracy in [9].

2.2.2 Position Estimation in $\mathbb{R}^3$

If the transmitters and the receiver reside in the Euclidian space $\mathbb{R}^3$ and each transmitter k has a known position in that space defined as $\mathbf{x}_k = [x_k, y_k, z_k]^T$ and estimate of the unknown position of the receiver in the space is made as $\hat{\mathbf{x}} = [\hat{x}, \hat{y}, \hat{z}]^T$, the distance between these two points can be determined using equation 2.1.

$$\hat{d}_k = \sqrt{(\hat{x} - x_k)^2 + (\hat{y} - y_k)^2 + (\hat{z} - z_k)^2} \tag{2.1}$$

The difference between the estimated distance $\hat{d}_k$ and the measured distance d_k provides a measure of how good the estimate $\hat{\mathbf{x}}$ is, and these differences form the components of a vector valued function $\mathbf{r}(\hat{\mathbf{x}}) = (r_1(\hat{\mathbf{x}}), r_2(\hat{\mathbf{x}}), \cdots, r_m(\hat{\mathbf{x}}))$, where each of the $r_k(\hat{\mathbf{x}})$'s is given by:

$$r_k(\hat{\mathbf{x}}) = d_k - \hat{d}_k = d_k - \sqrt{(\hat{x} - x_k)^2 + (\hat{y} - y_k)^2 + (\hat{z} - z_k)^2} \tag{2.2}$$

Each of the component functions of $\mathbf{r}(\hat{\mathbf{x}})$ is a function $r_k : \mathbb{R}^3 \mapsto \mathbb{R}$ for $k = 1, 2, \cdots, m$, and therefore $r : \mathbb{R}^3 \mapsto \mathbb{R}^m$. Consequently, this is a system of m equations in 3 unknowns. If $m > 3$ then the system is overdetermined and regression techniques can be used to calculate the unknown values.

Non-Linear Regression Techniques

The objective function that will be used is the sum of square residuals, given in equation 2.3.

$$f(\hat{\mathbf{x}}) = \frac{1}{2} \sum_{k=1}^{m} r_k^2(\hat{\mathbf{x}}) \tag{2.3}$$

It can be shown that equation 2.3 can be minimised via the following recurrence relation:

$$\hat{\mathbf{x}}_{i+1} = \hat{\mathbf{x}}_i - (\nabla^2 f(\hat{\mathbf{x}}_i))^{-1} \nabla f(\hat{\mathbf{x}}_i) \tag{2.4}$$

The Hessian matrix, $\nabla^2 f(\hat{\mathbf{x}}_i)$, is a matrix of all the second partial derivatives of the function $f(\hat{\mathbf{x}})$ calculated from the i^{th} estimate of $\hat{\mathbf{x}}$. An easier to compute, and commonly used, approximation of this matrix is $\nabla^2 f(\hat{\mathbf{x}}_i) \approx \mathbf{J_r}(\hat{\mathbf{x}}_i)^T \mathbf{J_r}(\hat{\mathbf{x}}_i)$, where $\mathbf{J_r}(\hat{\mathbf{x}}_i)$ is the Jacobian matrix of the residual vector function. This approximation is valid as long as the residuals are small and the function is close to linear near the solution. Using this approximation, equation 2.4 becomes equation 2.5.

$$\hat{\mathbf{x}}_{i+1} = \hat{\mathbf{x}}_i - (\mathbf{J_r}(\hat{\mathbf{x}}_i)^T \mathbf{J_r}(\hat{\mathbf{x}}_i))^{-1} \mathbf{J_r}(\hat{\mathbf{x}}_i)^T \mathbf{r}(\hat{\mathbf{x}}_i) \tag{2.5}$$

An improvement over the Gauss Newton method is the Levenberg-Marquardt (LM) algorithm, and this has become a common method of minimising equation 2.3. First developed in [10] this method has been used in a wide range of regression applications, including acting as the base algorithm for the work presented in [11] The update equation of the LM algorithm and can be expressed as follows:

$$\hat{\mathbf{x}}_{i+1} = \hat{\mathbf{x}}_i - \left(\mathbf{J_r}^T \mathbf{J_r} + \lambda \operatorname{diag}\left(\mathbf{J_r}^T \mathbf{J_r}\right)\right)^{-1} \mathbf{J_r}^T \mathbf{r}(\hat{\mathbf{x}}) \tag{2.6}$$

The use of the diagonalised $\mathbf{J_r}^T \mathbf{J_r}$ matrix multiplied by the scalar value λ, along with an appropriate rule for choosing the value of λ helps to ensure convergence of the algorithm if the residuals are larger, specifically it allows for more error in the initial estimate $\hat{\mathbf{x}}_0$.

The rule for updating λ is simple, if the sum of squared residuals has decreased since the last iteration then λ is decreased. If the sum of squared residuals has increased then λ is increased. That is, lambda decreases if the estimate is getting closer to the solution, and increased otherwise. The effect this has can be seen by examining equation 2.6.

If λ is zero then $\lambda \operatorname{diag}\left(\mathbf{J_r}^T \mathbf{J_r}\right)$ is zero and the equation becomes equation 2.4. If λ becomes large, then:

$$\left(\mathbf{J_r}^T \mathbf{J_r} + \lambda \operatorname{diag}\left(\mathbf{J_r}^T \mathbf{J_r}\right)\right)^{-1} \approx \left(\mathbf{J_r}^T \mathbf{J_r} + \lambda \mathbf{I}\right)^{-1} \approx \frac{1}{\lambda}\mathbf{I}$$

Consequently, equation 2.6 becomes a recurrence relation for the gradient descent method, which is far less sensitive to the magnitude of the residual, as it no longer features the Hessian approximation in a non-negligible form:

$$\hat{\mathbf{x}}_{i+1} = \hat{\mathbf{x}}_i - \frac{1}{\lambda}\mathbf{J_r}^T \mathbf{r}(\hat{\mathbf{x}}) \tag{2.7}$$

2.2.3 Robustness of These Techniques

The derivation of these techniques, specifically the assumptions made in the approximation $\nabla^2 f(x) \approx \mathbf{J_r}^T \mathbf{J_r}$, show that such regression techniques are very sensitive to magnitude of the residual vector. Thus if a d_k is input into the regression that creates a large error, the entire result can be effected and, in fact, the algorithm may diverge resulting in meaningless solutions.

The LM algorithm is an improvement over the GN algorithm in this respect, a large λ value will collapse the GN equation into gradient descent. Since the Hessian approximation is no longer an issue in this case a more liberal approach can be taken with regards to the signals that are sent to the regression. However, LM has no ability to ignore signals that are causing issues are therefore, while the solution may converge, it will do so with an unacceptable error, and give a meaningless output.

2.3 Robustness Against Reflection - The State of the Art

Methods for making least squares algorithms robust to ultrasonic reflections have been developed and presented in the literature, such as the method is presented in [11]. This study focuses on detecting outliers in the multilateration calculations and negating their effect on the final solution by use of an MM-estimator, an extension of the robust M-estimator. The M is an abbreviation of Maximum Likelihood, the repetition of the M in the extended version signifies that two M-estimates are used to increase robustness.

The MM-estimator is combined with a Least Trimmed Squares (LTS) method. In LTS the algorithm searches for the subset of the total data that produces the lowest least squares solution. This requires many regressions to take place, one for every subset, and is thus a fairly slow technique.

The number of regressions needed for a given number of reflections can be determined using the well known binomial coefficient.

$$\begin{pmatrix} a \\ k \end{pmatrix} = \frac{a!}{k!(a-k)!} \tag{2.8}$$

In equation 2.8, k represents the number of signals needed to calculate the position, i.e.:, the size of the subset, and a is the total number of signals received. It can be seen easily that the number of times the regression must be performed increases greatly with the number of reflections. In a system with four transmitters and 1, 2, 3, or 4 reflections present the system would require 5, 15, 35, or 70 regressions respectively. In systems that feature more transmitters the problem only increases; 8 transmitters and 4 reflections would require 495 regressions.

While robust regression techniques perform well at the task of outlier rejection, this performance requires a significant increase in computational cost. Additional contributions to this problem are shown in [12],

where a least median squares (LMedS) approach is taken, and [13] which is LTS based. Unfortunately the LMedS technique, like the LTS, uses comparisons of different subsets to work, and therefore inherits the above problem.

In order to address the problem of maintaining robustness while maximising efficiency, the authors in [12] develop a probabilistic technique to determine which of the subset combinations is most likely to be correct, thereby allowing their algorithm cut down on computation time by immediately rejecting unlikely combinations before the regression takes place.

The method in [12] uses the number of multiplications required as an indicator of the computational complexity of the algorithm. The complexity quoted by that paper is: $235LK + 280M$ for 10 iterations. Where L is the number of beacons chosen per subset for the LMedS technique, M is the total number of signals received and $K = {}^{M}C_{L}$, that is all the possible combinations. With $L = 3$, $K = 56$ and $M = 8$, as used in [12], this results in over 41,720 multiplications. While both [12] and [13] were developed for radio frequency system, the mathematics of regression is the same as for ultrasonic signals.

2.4 Conclusions

Methods for making ultrasonic localisation robust to reflections exist in the literature. However these methods all utilise subset searching techniques, resulting in a large computational cost, which it is desirable to avoid.

Since it is the subset searching technique which leads to the high computational cost it is proposed here to abandon such searching. Instead of an LTS or LMS approach, an iteratively reweighted least squares (IRLS) approach is adopted.

The proposed method is to use a combination of Bayesian probability and IRLS regression techniques in an ultrasonic localisation system to form a novel method of detecting and rejecting reflected ultrasonic signals with lower computational cost than state of the art methods.

Chapter 3

Current Progress

3.1 Introduction

This chapter will provide the reader with an overview of the current work that has been done towards the creation of the clinical measurement tool. As stated in chapter 1, the focus on of the project so far has been on the development of an algorithm to reject reflected ultrasonic signals. This is a major concern, and the development of this algorithm represents significant progress for the project and greatly increases the likelihood of achieving a successful outcome.

3.2 Processing the Received Signal

This algorithm works using a digital signal of the voltages recorded by the receiver. This signal was sampled a rate F_s in Hz and therefore has a period $T = \frac{1}{Fs}$ in seconds.

A frame is defined to be a window of the signal from the sample when transmitter 0 begins its n^{th} burst to the sample immediately before the same transmitter begins its $(n+1)^{th}$ burst. A block is defined to be a window of the n^{th} frame from the sample when the k^{th} transmitter begins its n^{th} burst to the sample immediately before the $(k+1)^{th}$ transmitter begins its n^{th} burst. A single frame, containing four blocks, is shown in figure 3.1.

Due to the size of the working volume of the system, the timing of the bursts and the speed of sound, each burst will have time to travel from its transmitter to the receiver before the next transmitter starts its burst.

This method will consider one frame at a time, and calculate a position from the information contained there, before processing to the next frame and calculating a second and so on. An algorithm can be employed to detect the received bursts, this algorithm will detect the LoS signals along with any NLoS signals of sufficient

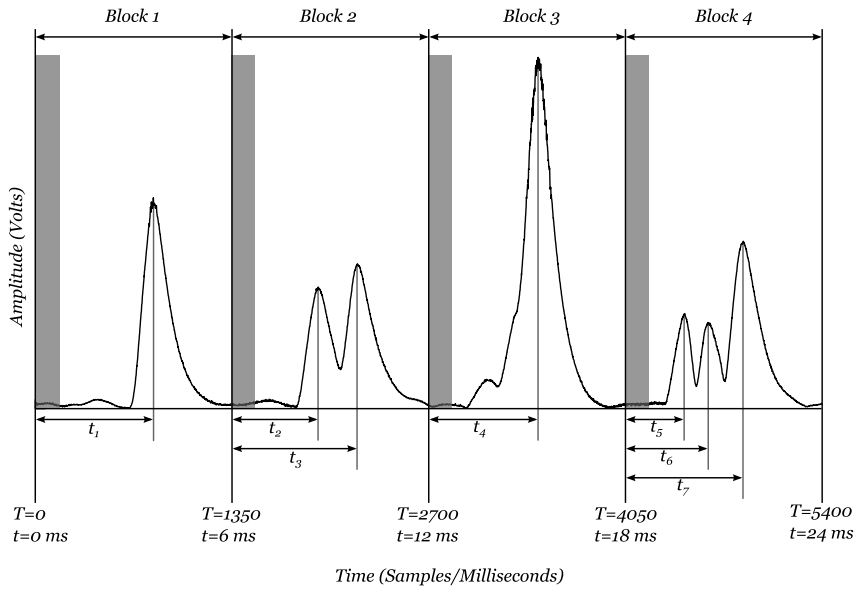

Figure 3.1: A typical input from an ultrasonic sensor over a single output cycle of four transmitters featuring multiple reflections, data has been processed by low pass filtering and envelope extraction using a Hilbert Transform. Time to peak values are indicated as well as the duration of the output signals (grey bars), block lengths are 1350 samples at 225kHz

amplitude. The time of flight will be calculated as discussed in section 2.2, t_0 for each signal will be the start time of the block the signal appeared in.

Therefore reflected NLoS signals will have a distance calculated for them that will be completely meaningless, the only purpose of this distance is to create a large error in the regression that can be used to identify the signal and reject it.

3.3 Bayesian Classification

The goal of classification is to determine which of a particular set of classes an object of interest belongs to. A signal's membership in a particular class is defined as $\phi \in \{0, 1\}$, where $\phi = 1$ if the signal is LoS and $\phi = 0$ otherwise. An estimate, $\hat{\phi}$, can be achieved using well known Bayesian techniques. Such methods are used in a wide variety of applications a good general overview of such techniques are given in [14, 15, 16].

Amplitude has been chosen as a suitable feature for this step based on the assumption that a multipath NLoS signal would have travelled further than a LoS signal, thus the amplitude should be diminished due to attenuation. However this cannot be guaranteed, and there are instances in which NLoS signals have a greater amplitude than LoS signals, therefore, classifying such signals based on their amplitude alone is ambiguous.

Due to this ambiguity, instead of directly classifying signals based on their amplitude, a Bayesian hypothesis

test is used, followed by a normalisation step to calculate probabilities that can later be used as weights in a regression step.

Let A be the event that the signal is LoS based on amplitude, let A^* be the event that the signal is NLoS. With s_i denoting the measured amplitude of the i^{th} received signal, the hypothesis test can be given as in equation 3.1. Where the likelihoods $p(s_i|A)$ and $p(s_i|A^*)$ are the probabilities that the signal i is LoS and NLoS respectively.

$$\hat{\phi}^{-}_{b_k|s_i} = p(A|s_i) = \frac{p(s_i|A)p(A)}{p(s_i|A)p(A) + p(s_i|A^*)p(A^*)} \tag{3.1}$$

The notation $\hat{\phi}^{-}_{b_k|s_i}$ denotes the probability calculated for the i^{th} signal in the k^{th} block. The superscript $-$ denotes that this probability is prior to the normalisation step, which is given by equation 3.2. This is used to ensure that all of the probabilities in each block sum to one.

$$\hat{\phi}_{b_k|s_i} = \frac{\hat{\phi}^{-}_{b_k|s_i} p(s_i)}{\sum_{j=1}^{n} \hat{\phi}^{-}_{b_k|s_j} p(s_j)} \tag{3.2}$$

The result, after this step, is a probability assigned to each signal in each block, based upon each signal's own amplitude and how its amplitude relates to the other signals in the block.

The likelihoods $p(s_i|A)$ and $p(s_i|A^*)$ in equation 3.1 are calculated from a pair of Gaussian probability density functions that attempt to model the distribution of LoS and NLoS amplitudes. This calculation is performed by numerically integrating each of the destiny functions over a small interval around the amplitude s_i of the signal. Here the region used was the interval $(s_i - 0.02, s_i + 0.02)$.

The mean and standard deviations of the probability density functions were generated by a combination of statistical analysis and some experience in dealing with the system. A random sample of experimental data was selected in which it was explicitly known which signals were LoS and NLoS. The amplitudes of each signal in each of the two categories were recorded and the means and standard deviations extracted.

Due to the shape of the Gaussian density function, if the mean is a positive value then there is part of the function that will return lower probabilities for amplitudes that are lower than the mean. Since this is not an effect that is desirable for this situation, after a process of trial and error it was found that better results could be achieved by setting the mean of the pdf for NLoS signals to zero and the standard deviations of each of the functions equal, thereby guaranteeing that the highest NLoS probabilities are generated by the signals with lowest amplitudes.

$p(A)$ is provided by a uniform probability mass function generated from the number of signals in the block. $p(A^*)$ is then the sum of the probability masses of everything that is not $p(A)$. For example, if there are three signals, the uniform distribution will give, for each signal, $p(A) = 1/3$ and $p(A^*) = 2/3$, for two signals

the priors would both be equal to one half.

3.4 Iteratively Reweighted Least Squares

To enable classification of signals during the regression an iteratively reweighted least squares (IRLS) method is used, with the update rule for the weights at each step taking into account the probabilities calculated earlier and the residual calculated in during the regression. The IRLS will be based on the LM algorithm 2.6, with the addition of a weight matrix giving equation 3.3.

$$\hat{\mathbf{x}}_{i+1} = \hat{\mathbf{x}}_i - \left(\mathbf{J}_\mathbf{r}^T\mathbf{W}\mathbf{J}_\mathbf{r} + \lambda \operatorname{diag}\left(\mathbf{J}_\mathbf{r}^T\mathbf{W}\mathbf{J}_\mathbf{r}\right)\right)^{-1}\mathbf{J}_\mathbf{r}^T\mathbf{W}\mathbf{r}(\hat{\mathbf{x}}) \tag{3.3}$$

A weight matrix is required, this will be initially populated with the probabilities calculated from the amplitudes of the signals.

The subscript $k|i$ = block|signal notation used in the probability step will be maintained here. $w_{k|i}$ is the weight of the i^{th} signal in the k^{th} block, while the block number may be different these are all, of course, part of the same matrix.

$$W = \begin{bmatrix} \hat{\phi}_{k=1|i=1} & 0 & \cdots & 0 \\ 0 & \hat{\phi}_{k=1|i=2} & & \vdots \\ \vdots & & \ddots & 0 \\ 0 & \cdots & & \hat{\phi}_{k=N_b|i=N_s} \end{bmatrix} \tag{3.4}$$

The initial weight matrix is shown in equation 3.4, where N_b is the number of blocks, and N_s is the number of signals in block $k = N_b$. Thus the probabilities are arranged in the order that their respective signals appear in the given frame. The update rule for the weights, defined with respect to a constant threshold value γ is given as:

$$w_{k|i} = \begin{cases} \dfrac{\gamma}{|r_{k|i}|}\hat{\phi}_{k|i} & \text{if} \quad |r_{k|i}| > \gamma \\ \\ 1 & \text{else} \end{cases} \tag{3.5}$$

The weight, updated in this way, allows for the probability calculated earlier to push the solution in the most probable direction, using a combination of probability based on amplitude and regression residual. The constant γ should be a small value in the expected range of error for the line of sight signals in the system. However, if the value is too small compared to the accuracy then the residual of a LoS signal may never reach the value, if it is too large then NLoS signals may have residuals less than it.

This system can take a long time to converge, in order to speed up the process a second weight update is implemented. The value of the individual weights can be further manipulated by taking into account the value of each residual compared to the other residuals of the same block.

Due to the timing of the transmitted signals, only one of the the signals in each block can be the LoS signal. This information can be leveraged to reach the result faster while minimising the negative effects this may have on the algorithm making an incorrect classification.

This works by detecting the minimum residual in each block (for blocks with more than one signal) and increasing the respective signals weight by multiplying it by a constant factor $q > 1$. The signal with the lowest residual is detected by the first part of equation 3.6. This signal then receives a slight boost in its weight, however, this boost is just a nudge in the right direction and is relatively small compared to the main re-weighing step shown in equation 3.5.

$$\begin{aligned} j &= \text{argmin}\{r_{k|i=1}, r_{k|i=2}, \cdots, r_{k|i=N_s}\} \\ w_{k|j}^{n+1} &= w_{k|j}^{n} q \end{aligned} \tag{3.6}$$

If $w_{k|j}^{n+1} > 1$, then this weight will be set to 1 before continuing. q itself is a constant value, and similar to γ, it also has a range of effective values. If it is too small it won't have any effect, and if it is too large it will cause the algorithm to become unstable. This study has found, through experiment, that $q = 2$ has a good effect in speeding up convergence without effecting stability.

3.5 Final Classification

Classification of the signals can be performed after convergence is achieved by classifying the signal in each block with the highest weight as the LoS signal. After this classification the regression can be continued as a standard regression with the NLoS signals removed.

This is done because some LoS signals may not have been fully weighted while some NLoS signals may still have a low, but non-zero, weight. These factors will effect the result of the regression if they are left in.

Attempts to further force the weights in either direction, down in the case of NLoS signals or up in the case of LoS signals, can have undesirable side effects, namely reducing the stability of the algorithm and causing divergence.

Utilising a hard classification at this point, and completely rejecting the signals currently classified as NLoS, ensures that there is no undue influence of either NLoS signals with non-zero weight or LoS signals with a weight less than one.

The progress made by the algorithm while classifying the signals need not be lost, and when the algorithm is restarted it can begin at the last estimate of the parameters that were calculated before the hard classification was performed. Furthermore, because the only signals left will be the LoS signals and the parameter estimates will already be close to the true solutions, the regression can be continued with a pure Gauss Newton method without need for the additional complexity of the Levenberg-Marquardt algorithm.

3.6 Computational Complexity

The method developed here is an iteratively reweighted LM algorithm that eliminates the need for the subset searching method used in [12]. This creates a difference in the computational cost of the two algorithms. In order to eliminate the multiple regressions required by [12] the proposed method uses a Jacobian matrix with a number of rows equal to the number of signals received, i.e.: a matrix of variable dimension, causing the computational cost of the matrix algebra to be dependent on the number of signals received.

These two techniques will now be compared to show that the proposed method can find solutions at a lower computational cost than the method outlined in [12].

Using a to represent the total number of received signals and p as the number of parameters to be estimated, the number of multiplications required per iteration is given in equation 3.7.

$$p^3 + a^2p + ap^2 + ap + a \tag{3.7}$$

a^2p is the number of multiplications required to multiply the transposed Jacobian by the weight matrix, and ap^2 multiplications are needed to multiply this again by the Jacobian to obtain the $\mathbf{J}^T\mathbf{W}\mathbf{J}$ Hessian approximation which will always be a $p \times p$ matrix, for which p^3 multiplications are needed to find the inverse. ap is required to multiply the already obtained $\mathbf{J}^T\mathbf{W}$ by the residual and finally a linear factor of a is required to for the probability calculations.

Since the number of parameters, x, y, z, being estimated is a constant 3 the expression in 3.7 can be reduced to the expression shown in equation 3.8.

$$3a^2 + 13a + 27 \tag{3.8}$$

As an example: for total of 8 and 16 received LoS and NLoS signals, this method requires 6,460 and 20,060 multiplications for 20 iterations, respectively, compared to the 41,720 for 8 signals in [12].

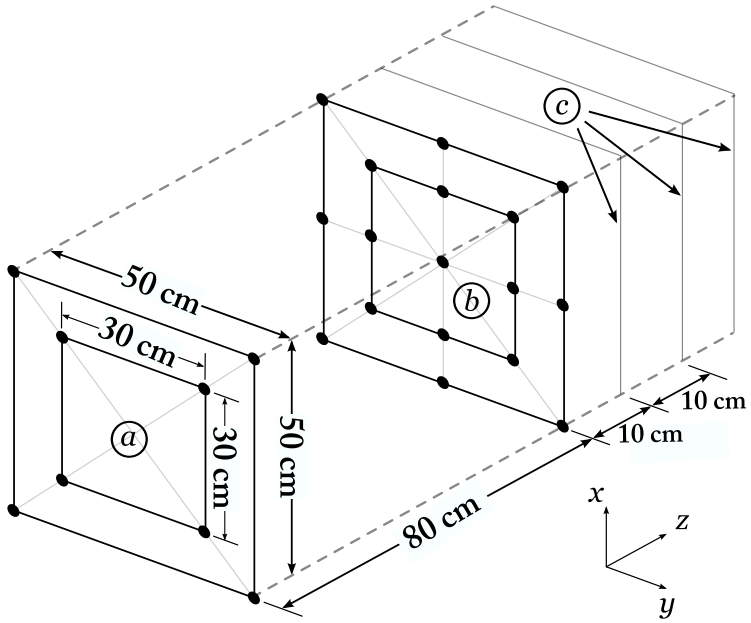

Figure 3.2: Experimental Set Up Diagram Showing: a) Transmitter Plane, b) Receiver Plane in Initial Position 80 cm from Transmitter Plane, c) Incremented Positions of Receiver Plane

3.7 Experimental Work

In order to test the validity of the IRLS algorithm as well as to illustrate how it works, the method has been tested on data collected during experiments. To demonstrate how well the method works, results will be presented summarising the performance of the method across all the data available, and results will also be presented for a specific case in order to illustrate the details of how the method performs.

The algorithm as it has already been described requires a number of parameter values to be specified before the program is used. These maybe constants or values that change every iteration, but require user specified initial values. These parameters and the values used in the tests are presented in table 3.1.

3.7.1 Experimental Set Up

The algorithm has been tested on data collected during a series of experiments. These experiments investigated different configurations of transmitters and receivers. A diagram of the set up can be seen in figure 3.2.

Two square, planar configurations of four transmitters were tested, with edge lengths of 30 cm and 50 cm respectively, (a) in figure 3.2. The receivers were placed into a similar board, but with a more varied configuration, (b) in figure 3.2. The receiver positions had the same 30 cm and 50 cm square configuration, while also having positions on the midpoints of the lines between the square positions and one at the center

of the overall configuration.

Both the transmitter and receiver configurations were achieved by placing the transducers in appropriately positioned holes in plywood boards. These boards were mounted upon supports, to raise them from the ground. The two planes were connected by a rail on the ground, to ensure that the relative positions of transmitters and receivers could be easily controlled and measured.

Experiments were performed both with and without acoustically absorbent foam padding covering the plywood board holding the receivers.

The transmitters and receivers used in this experiment were Prowave 328ST160 and 328SR160 respectively, these transducers have a center frequency of 32.8 kHz.

The transmitted signals were passed through a Texas Instruments THS6012 Amplifier and the received signal was conditioned using an Alligator Technologies USBPIA-S1 programmable instrumentation amplifier before being delivered to the analog-to-digital converter.

A Data Translation DT9836 series simultaneous DAQ module was used for output of the driving signals from MATLAB and recording the incoming signals from the receivers. The simultaneous input and output sampling of this module allowed for the transmitters and receivers to the fully synchronised in time with the use of a hardware trigger to start all input and output channels at the same time.

Table 3.1: Initial Parameter Values

Parameter Name	**Notation**	**Init. Val.**	**Unit**	**Constant**
NLoS pdf mean	μ_{NLoS}	0	Volts	Yes
NLoS pdf standard deviation	σ_{NLoS}	0.35	Volts	Yes
LoS pdf mean	μ_{LoS}	0.71	Volts	Yes
LoS pdf standard deviation	σ_{LoS}	0.35	Volts	Yes
Initial Marquardt Parameter	λ	1	None	No
Marquardt Criterion	λ_C	0.001	None	Yes
Marquardt Increment	λ_I	2	None	Yes
Weight Update Threshold	γ	0.01	None	Yes
Fast Convergence Nudging Factor	q	2	None	Yes
Initial Guess for x	$\hat{x}_0$	0	metres	No
Initial Guess for y	$\hat{y}_0$	0	metres	No
Initial Guess for z	$\hat{z}_0$	1	metres	No

3.7.2 Experimental Method

With the four transmitters in the 30 cm square configuration and the receiver board positioned 80 cm from the transmitter board a train of signals were set from each of the transmitters for a duration of 1 second.

The data from each of the four receivers was recorded into MATLAB simultaneously.

Six different single frequency amplitude modulated signals were tested: square, trapezoid, triangle and sawtooth envelopes were used as well as two amplitude modulated chirp signals with bandwidths of 10 kHz and 15 kHz.

3.8 Experimental Results

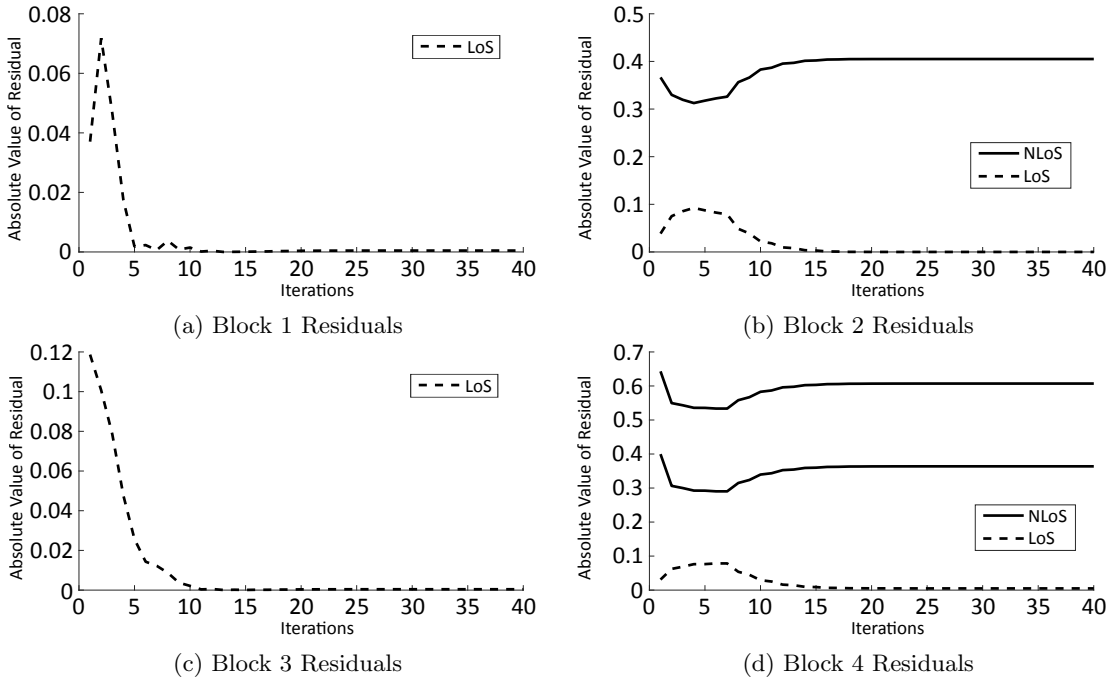

(a) Block 1 Residuals

(b) Block 2 Residuals

(c) Block 3 Residuals

(d) Block 4 Residuals

Figure 3.3: Residuals by block from a single regression

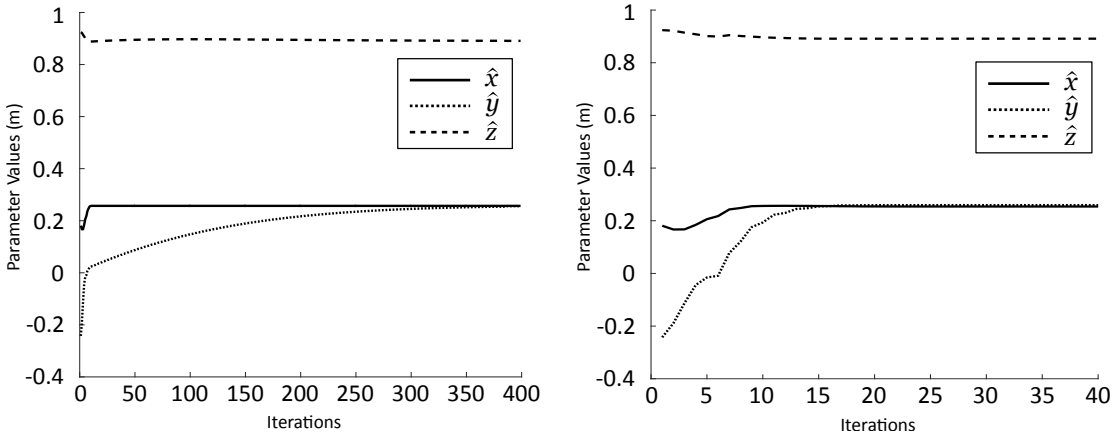

(a) Regular Convergence of Parameters $\hat{x}, \hat{y}, \hat{z}$ (0 - 400 Iterations)

(b) Fast Convergence of Parameters $\hat{x}, \hat{y}, \hat{z}$ (0 - 40 Iterations)

Figure 3.4: Comparison of parameter convergence

Table 3.2: NLoS Classification Results Without Acoustic Padding

Envelope Type	**Correct NLoS Classification**	**Incorrect Classification**	**% Correctly Classified**
Square	4543	22	99.5
Trapezoid	4928	34	99.3
Triangle	5178	132	97.5
Sawtooth	5072	160	96.9
Chirp 10 kHz	6544	558	91.8
Chirp 15 kHz	11986	2766	79.3

Table 3.3: NLoS Classification Results With Acoustic Padding

Envelope Type	**Correct NLoS Classification**	**Incorrect Classification**	**% Correctly Classified**
Square	297	0	100
Trapezoid	407	0	100
Triangle	419	0	100
Sawtooth	414	0	100
Chirp 10 kHz	1379	52	96.3
Chirp 15 kHz	51574	15098	74.4

General Classification Results

Tables 3.2 and 3.3 show the algorithms ability to classify signals over the entire dataset.

General Accuracy Results

Tables 3.4 and 3.5 show the accuracy of the 1D distances and 3D positions calculated by the algorithm.

3.9 Discussion of Results

Analysing the residuals of the signals by block, as presented in figures 3.3a to 3.3d, gives an insight into how the algorithm is working. Firstly it can be seen that for those blocks that contain only one signal, figures 3.3a and 3.3c, the residual converges very quickly to near zero.

In the blocks with more than one signal, figures 3.3b and 3.3d, the LoS signal always has a lower residual than that of the NLoS signals, which is as expected. Also the residuals of the NLoS signals increase over

Table 3.4: Measurement Error in Millimetres From all Experiments With Acoustic Padding

Envelope Type	**1D/3D**	**Mean**	**Std. Dev.**	**Max.**	**Min.**
Square	1D	0.61	6.49	21.44	-19.19
Square	3D	2.92	7.33	27.66	-10.03
Trapezoid	1D	0.67	6.19	21.59	-16.14
Trapezoid	3D	5.41	4.19	22.22	0.06
Triangle	1D	0.38	6.35	21.58	-19.44
Triangle	3D	4.91	3.77	22.00	0.01
Sawtooth	1D	9.23	5.67	27.95	-10.74
Sawtooth	3D	11.85	8.76	39.25	-13.57
Chirp 10 kHz	1D	-26.01	10.57	36.04	-50.02
Chirp 10 kHz	3D	28.86	8.44	61.77	6.56
Chirp 15 kHz	1D	-32.63	11.28	40.48	-59.01
Chirp 15 kHz	3D	35.76	9.34	69.24	8.41

Table 3.5: Measurement Error in Millimetres From all Experiments Without Acoustic Padding

Envelope Type	**1D/3D**	**Mean**	**Std. Dev.**	**Max.**	**Min.**
Square	1D	-2.32	13.81	68.35	-37.95
Square	3D	-2.68	8.84	38.38	-10.03
Trapezoid	1D	-0.69	13.73	68.29	-46.53
Trapezoid	3D	8.68	8.83	48.37	0.03
Triangle	1D	-0.57	16.29	143.39	-47.62
Triangle	3D	8.68	8.84	48.38	0.03
Sawtooth	1D	8.33	14.7	170.38	-34.02
Sawtooth	3D	9.14	11.81	55.75	-20.49
Chirp 10 kHz	1D	-25.97	20.79	138.50	-66.17
Chirp 10 kHz	3D	31.12	8.99	61.21	2.39
Chirp 15 kHz	1D	-32.36	21.85	81.27	-73.64
Chirp 15 kHz	3D	35.98	10.67	65.57	0.61

time before converging to some value $r \gg 0$ whereas the residual for the LoS signal degreases gradually. Although the residual for the LoS signal in multi-signal blocks does not converge as close to zero as in the blocks with only one signal, it ends up far closer to zero than the residuals of NLoS signals.

Tables 3.2 and 3.3 show that the best results are obtained with the Square, Trapezoid, Triangle and Sawtooth enveloped signals, both chirp signals show the worse performance owing to distortion of the high-bandwidth signal by the narrow-bandwidth transducers used.

The method for calculating the time of flight from the received ultrasonic bursts has been developed with a focus on the square, trapezoid, triangle, and sawtooth waveforms. Although each of these envelope shapes are different when transmitted, they do have a very similar general envelope shape when received. The distorted chirp signals have a greater difference in shape and quality, which presents a greater challenge for the very simple peak finding algorithm.

With the chirp signals, spurious peaks caused by random noise are likely to be identified as possible signals in the same way as both the received LoS and NLoS signals. The incorrect identification of noise as a signal in these cases greatly increases the difficultly for the NLoS rejection algorithm in the regression stage.

The effect of random noise is greater close to the amplitude peak, where the slope of the envelope is near zero, this phenomena is one of the main challenges in estimating time of flight from time of maximum amplitude. In cases where it is far enough away from the peak to be considered as a possible signal, but also close enough to correspond to a time of flight similar to that of the LoS signal. The large number of detected signals in the experiments with chirps, due to numerous large noise created peaks, also makes it difficult to find the true LoS signal.

3.9.1 Bayesian Probability Step

The probability distributions used to calculate the probability in the Bayesian step were a pair of Gaussian distributions. These have worked very well during the tests, given that their standard deviations were calculated from a very limited quantity of data.

Other distributions may outperform the Gaussian, but these have not been considered here. The role of the distribution is to give a very rough estimate for the regression step to refine.

The regression step is where the bulk of the classification work is handled and as a result this allows a slightly relaxed approach to choosing these distributions.

However the failure shown in table 3.2, for the envelopes other than the chirp signals, all occurred while attempting to classify the signals in the experiments with 1.2 and 1.3 metre distance between receiver and transmitter planes.

At these distance the signal amplitude will be lower due to attenuation. As the density functions used

in the hypothesis test remain fixed, but the amplitudes of both LoS and NLoS signals become lower, the probabilities calculated from these density functions will generate higher NLoS probabilities, $p(x_i|A^*)$, than LoS probabilities $(x_i|A)$, for all signals. Improvements could be made by implementing an adaptive scheme that scales the distributions based on the calculated distance, to stop the probability step being effected in this way be attenuated signals.

3.9.2 Fast Convergence

Figure 3.4b shows the fast convergence algorithm working. By comparing figures 3.4a and 3.4b it can be seen that convergence time is reduced drastically whilst obtaining the same result.

In figure 3.4a the parameters $\hat{x}, \hat{y}, \hat{z}$ do converge and approach the true values. However, they take a long time to get there, nearly 400 iterations. The result in 3.4b shows a vast improvement, convergence is achieved in 15 to 20 iterations.

This result is consistent throughout the experimental data, all examples with successful classifications converge in less than 20 iterations.

Chapter 4

Future Work

A second experiment has been performed since the one discussed in the report so far. This experiment used 8 transmitters instead of 4, which were held in to two perpendicular planes. The purpose of this experiment was to investigate the effect of signal blockage due to obstacles. Two 150 mm diameter cylinders were used to block signals by placing them in different positions between the transmitters and receivers.

Although the experiment has been conducted, it still remains to analyse the data recorded. This analysis will reveal the effect that these obstacles has caused the systems ability to calculate the position of the receiver.

The algorithm that has been discussed in this report will need to be be expanded and improved to mitigate the effect of signal blockage. While the IRLS method may be able to cope with some cases of obstacles, it works from an assumption that there will be one line of sight signal in each block, which cannot be guaranteed if there is a possibility of signal blockage. The extent of the modification that is required will not be known until this analysis has been conducted.

In addition to the development of an obstacle mitigation algorithm, it is also necessary to implement a more sophisticated method of time of arrival estimation. Currently the method being used is based on basic peak detection, which creates errors which are non acceptable for this application. Many techniques for this already exist and it therefore may not be necessary to develop a novel technique to perform this function. In order to determine this an analysis of current methods of time of arrival estimation will be conducted on the data that has been collected to date.

Once techniques for obstacle mitigation and time of arrival estimation have been developed and implemented alongside the reflection rejection method, the result will be a robust and accurate ultrasonic localisation platform.

This platform will then need to be tested for its suitability in measuring anatomical landmarks. This can be done by using the ultrasonic platform to collect point measurements from a phantom model of a spine, and comparing these measurements to those collected by other measurement techniques.

This testing will allow for the validation of the measurement device, in the case that it works well. If the device does not function as desired, the information gained from this testing can be used to help refine and improve the system.

Figure 4.1 show a Gantt chart of the plan for completing the work outlined where over the course of the next year.

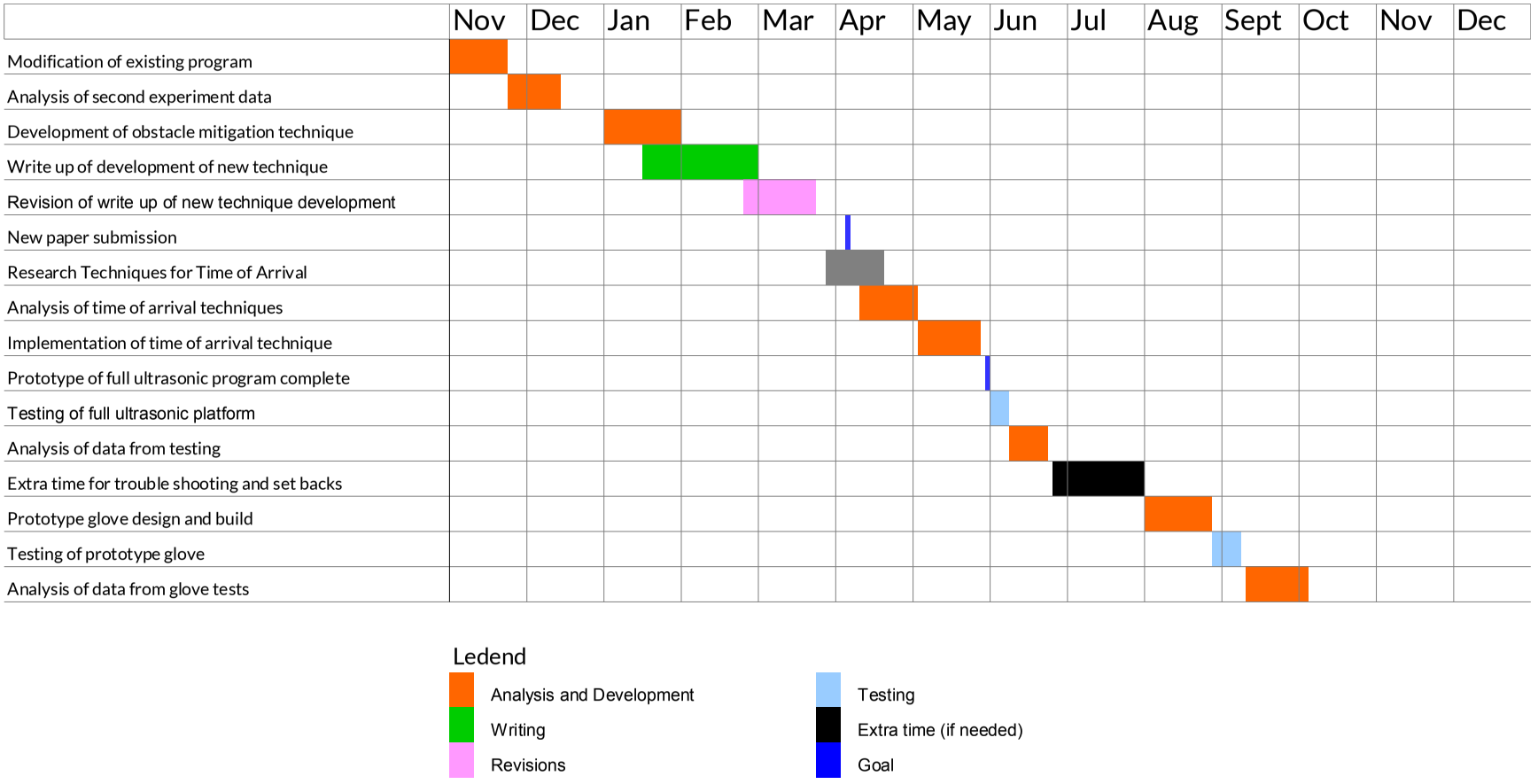

Figure 4.1: Gantt Chart

Chapter 5

Conclusion

An outline of the current progress towards the completion of the project has been presented. Two sets of experiments have been conducted, each designed to thoroughly investigate two major problems that can occur in ultrasonic positioning, namely reflections and signal blockage due to obstacles.

One set of experimental data has been analysed and a novel technique for the rejection of NLoS, reflected signals has been developed which performs well, even with highly distorted and noisy signals, while having a reduced computational cost compared to the existing state of the art. This represents a major milestone for the project, and is forms a foundation from which the remainder of the system can be developed.

A clear plan has been presented for future work, including the analysis of the data from the second experiment and the further development and completion of the ultrasonic localisation system.

Bibliography

[1] M. Khalkhali, M. Parnianpour, H. Karimi, B. Mobini, and A. Kazemnejhad, "The validity and reliability of measurement of thoracic kyphosis using flexible ruler in postural hyper-kyphotic patients," *Journal of Biomechanics*, vol. 36, p. S541, 2006.

[2] F. D'Osualdo, S. Schierano, and M. Iannis, "Validation of clinical measurement of kyphosis with a simple instrument, the arcometer," *Spine*, vol. 22, pp. 408–413, 1997.

[3] F. Chaise, C. Candotti, M. Torre, T. Furlanetto, P. Pelinson, and J. Loss, "Validation, repeatability and reproducibility of a noninvasive instrument for measuring thoracic and lumbar curvature of the spine in the sagittal plane," *Brazilian Journal of Physical Therapy*, vol. 15, pp. 511 – 517, 2011.

[4] G. Greendale, N. Nili, M. Huang, L. Seeger, and A. Karlamangla, "The reliability and validity of three non-radiological measures of thoracic kyphosis and their relations to the standing radiological cobb anglealidation, repeatability and reproducibility of a noninvasive instrument for measuring thoracic and lumbar curvature of the spine in the sagittal plane," *Osteoporosis International*, vol. 22, pp. 1897 – 1905, 2011.

[5] J. Sedrez, C. Candotti, T. Furlanetto, and J. Loss, "Non-invasive postural assessment of the spine in the sagittal plane: a systematic review," *Motricidade*, vol. 12, pp. 140 – 154, 2016.

[6] M. Parrilla, J. Anaya, and C. Fritsch, "Digital signal processing techniques for high accuracy ultrasonic range measurements," *IEEE Transactions on Instrumentation and Measurement*, vol. 40, no. 4, pp. 759–763, 1991.

[7] L. Angrisani and R. Schiano Lo Moriello, "Estimating ultrasonic time-of-flight through quadrature demodulation," *IEEE Transactions on Instrumentation and Measurement*, vol. 55, no. 1, pp. 54–62, 2006.

[8] R. Raya, A. Frizera, R. Ceres, L. Calderón, and E. Rocon, "Design and evaluation of a fast model-based algorithm for ultrasonic range measurements," *Sensors and Actuators, A: Physical*, vol. 148, no. 1, pp. 335–341, 2008.

[9] S. Jiang, C. Yang, R. Huang, C. Fang, and T. Yeh, "An Innovative Ultrasonic Time-of-Flight Measurement Method Using Peak Time Sequences of Different Frequencies: Part I," *IEEE Transactions on Instrumentation and Measurement*, vol. 60, no. 3, pp. 735–644, 2011.

[10] D. W. Marquardt, "An Algorithm for Least-Squares Estimation of Nonlinear Parameters," *Journal of the Society for Industrial and Applied Mathematics*, vol. 11, no. 2, pp. 431–441, 1963.

[11] J. C. Prieto, C. Croux, and A. R. Jiménez, "RoPEUS: A new robust algorithm for static positioning in ultrasonic systems," *Sensors*, vol. 9, no. 6, pp. 4211–4229, 2009.

[12] T. Qiao and H. Liu, "Improved Least Median of Squares Localization for Non-Line-of-Sight Mitigation," *IEEE Communication Letters*, vol. 18, no. 8, pp. 1451–1454, 2014.

[13] J. Khodjaev, S. Tedesco, and B. O. Flynn, "Improved NLOS Error Mitigation Based on LTS Algorithm," *Progress In Electromagnetics Research Letters*, vol. 58, no. October 2015, pp. 133–139, 2016.

[14] N. Friedman, D. Geiger, and M. Goldszmit, "Bayesian Network Classifiers," *Machine Learning*, vol. 29, pp. 131–163, 1997.

[15] W. T. Freeman and D. H. Brainard, "Bayesian decision theory, the maximum local mass estimate, and color constancy," *Proceedings of IEEE International Conference on Computer Vision*, pp. 210–217, Jun 1995.

[16] Y. Ephraim, "A Bayesian Estimation Approach for Speech Enhancement Using Hidden Markov Models," *IEEE Transactions on Signal Processing*, vol. 40, no. 4, 1992.